Luminescence chronology of the northeastern Bulgarian loess-paleosol sequences (Viatovo and Kaolinovo)

Sanda Balescu, Diana Jordanova, Laurence Forget Brisson, François Hardy, Sébastien Huot, Michel Lamothe

Luminescence chronology of the northeastern Bulgarian loess-paleosol sequences (Viatovo and Kaolinovo)

Sanda BALESCU[1], Diana JORDANOVA[2], Laurence FORGET BRISSON[3], François HARDY[3] Sébastien HUOT[4], Michel LAMOTHE[3]

[1] *Université de Lille, Laboratoire Halma (UMR 8164, CNRS), Bâtiment de Géographie, 59655 Villeneuve d'Ascq Cedex, France*

[2] *National Institute of Geophysics, Geodesy and Geography, Bulg. Acad. Sci., Acad. G. Bonchev bl.3, 1113 Sofia, Bulgaria*

[3] *Université du Québec à Montréal, Département des Sciences de la Terre et de l'Atmosphère, Laboratoire de luminescence LUX, H3C 3P8 Montréal, Canada*

[4] *Illinois State Geological Survey, Prairie Research Institute, University of Illinois at Urbana-Champaign, USA*

Abstract

The key reference loess sequence of Viatovo in NE Bulgaria, lying within the lower Danube basin, records climatic and environmental changes over the last 800 ka. This 20 m thick loess sequence consists of seven loess units (L1 to L7) intercalated by six paleosols (S1 to S6) below the modern soil (S0). The Matuyama-Brunhes palaeomagnetic boundary has been identified in the lowest loess unit (L7). This reference loess sequence remains so far undated by radiometric techniques. Its chronostratigraphy relies only on pedostratigraphic and magnetostratigraphic evidence. This contrasts with the adjacent reference loess sequences of SE Romania (Tuzla, Mostistea, Mircea Vodă) whose luminescence chronology is now securely established up to MIS 8.

The aim of this study is to validate the chronostratigraphic framework of the Viatovo loess sequence using the luminescence dating method. For this purpose, the luminescence method is applied to the three upper loess units (L1, L2, L3) from two adjacent sites: the reference site of Viatovo and the nearby site of Kaolinovo, both located in the Ludogorie region (NE Bulgaria) and showing the same superposition of loess (L1 to L7) and interbedded paleosols. Luminescence dating (Infrared stimulated luminescence; IRSL) was carried out using the feldspar fine sand-size grain fraction (60-80 μm), applying the $IRSL_{50}$ and the $pIRIR_{290}$ dating techniques. For the equivalent dose (De) determination we used both the SAR post-infrared infrared ($pIRIR_{290}$) protocol on single aliquots and the multiple-aliquot additive dose (MAAD $IRSL_{50}$) protocol. The $pIRIR_{290}$ ages and the fading corrected MAAD-$IRSL_{50}$ ages are self-consistent. It demonstrates for the first time, that the three upper loess layers (L1, L2, L3) at Viatovo and Kaolinovo were deposited during the marine isotope stages (MIS) 2-4, 6 and 8, thus constraining the youngest well-developed paleosol (S1, a chernozem) to the Last Interglacial. These $IRSL_{50}$ and $pIRIR_{290}$ ages are in good agreement with the luminescence ages obtained for (1) the two upper loess layers (L1, L2) from the Harletz sequence in NW Bulgaria and (2) the three upper loess units (L1, L2, L3) from the adjacent SE Romanian loess sequences.

The luminescence chronology of the loess sequences is presented along with the pedogenic and magnetic property data. The pedostratigraphic records of the NE Bulgarian and SE Romanian loess sequences show the same palaeoclimatic trends, with progressive aridification during interglacial periods (from S6 to S0).

Key words: Loess, Pleistocene, IRSL dating, K-feldspars, Bulgaria, Romania
Corresponding author: Tel: + 33 686009269
E-mail address: sanda.balescu@univ-lille.fr (S. Balescu)

1. Introduction

The loess-paleosol sequences from NE Bulgaria and SE Romania, both lying within the lower Danube basin (Fig. 1A) are among the thickest (Haase et al., 2007) and most complete southeastern European terrestrial palaeoclimatic archives. These 20 to 30 m thick loess-paleosol sequences record climatic and environmental changes over the last 800 ka. The Matuyama-Brunhes palaeomagnetic boundary (MBB) has been identified in the lowest loess unit both in NE Bulgaria, at Viatovo (Jordanova et al., 2008) and in SE Romania, at Tuzla (Balescu et al., 2003) and Zimnicea (Radan, 2012) (Fig. 1B). These loess deposits have an aeolian origin (Smalley and Leach, 1978; Evlogiev, 2007; Smalley et al., 2009) and their source material is mostly derived from the alluvium of the lower Danube valley, with additional dust transported from the outwash of the northern Fennoscandian ice sheet (Evlogiev, 2007; Buggle et al., 2008; Fitzsimmons et al., 2012; Kis et al., 2012; Jipa, 2014) and minor components from the Sahara (Stuut et al, 2009).

The reference loess sequences of Viatovo and Koriten in NE Bulgaria (Fig. 1B), well known for their most complete paleomagnetic records (Jordanova and Petersen,1999a,b; Jordanova et al. 2008), consist of seven loess layers (named L1 to L7 from top to bottom, following the stratigraphic nomenclature adopted by Jordanova et al. (1999a,b) for the Bulgarian loess) and six intercalated paleosols (named S1 to S6) below the recent (Holocene) soil (S0) (Fig. 2). However, these remain so far undated by radiometric techniques. Their chronostratigraphy relies only on geomorphic, pedostratigraphic and magnetostratigraphic evidence (Jordanova and Petersen,1999a,b; Jordanova et al. 2008). This contrasts with the adjacent SE Romanian reference loess sequences of Tuzla, Mostiştea and Mircea Vodă (Fig. 1B) whose chronology is now securely established by luminescence dating up to MIS 8 (Balescu et al., 2003, 2010; Timar et al., 2010, Timar-Gabor et al., 2011; Vasiliniuc et al., 2011, 2012, 2013).

The aim of the present study is to provide the first chronological framework for the Viatovo reference loess-paleosol sequence using the luminescence dating method in order to validate the magnetostratigraphy-based age model established by Jordanova and Petersen (1999a,b) and Jordanova et al. (2008) at Viatovo and Koriten.

For this purpose, the luminescence dating method (Infrared stimulated luminescence; IRSL) is applied herein to the three upper loess layers (L1, L2, L3) from the Viatovo loess-paleosol sequence (Jordanova et al, 2008; Kis et al. 2012) and the nearby long loess sequence of Kaolinovo (Fig. 2) which shows the same superposition of loess (L1 to L7) and interbedded paleosols. It could not be tested on the reference loess sequence of Koriten (Jordanova and Petersen (1999a,b) which is unfortunately no longer accessible.

Since the quartz OSL (*optically stimulated luminescence*) dating method applied to the NW Bulgarian and SE Romanian loess is limited to the last 70-100 ka (Timar et al., 2010; Timar-Gabor et al., 2011; Lomax et al., 2018), we focus herein on K-feldspars whose luminescence signals saturate at much higher doses and thus have the potential to date much older sediments. In the present study, we apply both the post-infrared infrared ($pIRIR_{290}$) (Thomsen et al., 2008; Buylaert et al., 2012) and the $IRSL_{50}$ dating techniques to K-feldspar fine sand-size (60-80 μm) grains from the three upper loess layers (L1, L2, L3). These ages will be further compared with the luminescence ages obtained for (1) the two upper loess layers (L1, L2) from the Harletz sequence (Fig. 1B) in NW Bulgaria (Lomax et al., 2018) and (2) the three upper loess units (L1, L2, L3) from the adjacent SE Romanian loess sequences in order to better ascertain the regional stratigraphic correlations of the Pleistocene loess deposits across the lower Danube basin.

In this study, the luminescence chronologies of the NE Bulgarian and SE Romanian loess sequences are presented along with the pedostratigraphic and magnetic susceptibility data which provide important information on the palaeoclimatic evolution of the lower Danube basin during the Pleistocene.

2. Study sites and sampling

The Viatovo and Kaolinovo loess sequences are located at the southern fringe of the Lower Danube Basin (Fig. 1B). They are situated between the Danube and the Balkan Mountains, in the Ludogorie region (Fig. 1B), which is characterized by a hilly relief with deeply incised river valleys (Zagorchev, 2009). The average elevation of the region is 200-300 m asl. This region is lying next to the Dobrogea plateau (Fig 1B) which extends from NE Bulgaria to SE Romania, along the Black Sea coast, and culminates at 300 m asl. The reference loess sequence of Koriten (Jordanova and Petersen, 1999a,b) located in this area is no longer accessible.

The Ludogorie and Dobrogea regions, both preserve some of the thickest and most complete loess sequences of the lower Danube Basin. The Bulgarian loess deposits are the thickest (30-40 m) close to the Danube and are thinning southwards, toward the Fore Balkan (Evlogiev, 2007). The grain-size of the loess is also gradually decreasing from the Danube alluvial plain toward the Fore Balkan (Evlogiev, 2007).

The Viatovo and Kaolinovo loess-paleosol sequences are exposed on the walls of active quarries where Albian - Early Eocene sandy kaolinitic deposits are being extracted (Tonov et al., 2016). The sedimentary complex lying on top of these deposits is represented by a 6-8 m thick Pliocene red clay formation (terra rossa) overlain by a loess-paleosol sequence of a 20 m

thickness, consisting of seven loess layers (L1-L7) and six interbedded paleosols (S1-S6) (Fig. 2). The paleosols and loess layers recognized in the field are numbered and designated S and L, respectively, according to the original stratigraphic nomenclature adopted by Jordanova and Petersen (1999a,b) for the Bulgarian loess and later extended to the Romanian loess by Panaiotu et al. (2001). This nomenclature complies with the unified Danube loess stratigraphic model recently proposed by Marković et al. (2015).

The chronostratigraphy of the Viatovo and Kaolinovo loess sequences relies on geomorphic, pedostratigraphic and magnetostratigraphic evidence. A chronostratigraphic framework has been established on the basis of the detailed magnetic susceptibility (MS) records of the Koriten and Viatovo loess-paleosol sequences (Jordanova and Petersen,1999a,b; Jordanova et al., 2007, 2008). The MS signatures of these loess-paleosol sequences have been correlated with the astronomically tuned ODP677 $\delta^{18}O$ record of Shackleton et al. (1990). The age of the oldest loess deposit (L7) is constrained palaeomagnetically at Viatovo by the identification of the Brunhes-Matuyama palaeomagnetic boundary (MBB: 772 ± 7 ka according to Sugunama et al., 2015; following the nomenclature system adopted by Fitzsimmons et al., 2012 and Marković et al., 2015) thus yielding a maximum age limit for these loess deposits (Jordanova et al., 2008).

The **Viatovo** loess section (Fig. 2, Fig. S1) (43° 41' 18.6" N; 26° 14' 48.6" E; 219 m a.s.l) is a key reference site for the Bulgarian loess, being well-known for its most complete palaeomagnetic record. The mineralogy, grain-size and magnetic mineral characteristics of this loess-paleosol sequence were previously investigated (Jordanova et al., 2007, 2008; Kis et al., 2012). It has a thickness of 21 m. A short description of each loess unit is presented in Table S1. The recent (Holocene) soil (S0) is a dark gray soil (B-horizon). The first three paleosols (S1-S3) are dark brown chernozem-like (steppe) soils associated with dry climatic conditions (Fotakieva, 1974; Minkov, 1968; Eckmeier et al., 2007). The older paleosols (S4-S6) are red, rubified, clay-rich forest soils that developed in a warmer and more humid climate (Jordanova et al., 2008).

MBB has been identified at Viatovo, in loess L7 (Fig. 2). Moreover, two normal polarity magnetozones have been discovered in the underlying red clay formation corresponding to the Jaramillo and Olduvai subchronozons (Jordanova et al., 2008).

The **Kaolinovo** section (Fig. 2, Fig. S2) (43° 35' 52" N; 27° 09' 26.7" E; 253 m asl) has a total thickness of 20.3 m. A short description of each loess unit is presented in Table S2. The recent soil S0 is represented by a moderately leached Chernozem. The first three paleosols (S1-S3) are dark brown chernozem-like (steppe) soils (Fig. S2). The older paleosols (S4-S6) are reddish soils.

The stratigraphy and the IRSL sampling positions are shown in Figure 2. The present study focuses on seven IRSL samples collected within the three uppermost loess layers (L1, L2, L3) both at Viatovo (VIA 1,2,3) and Kaolinovo (KA 1, 2, 3) and, in the oldest loess (L7) at Viatovo, below the MBB (VIA 7). The IRSL technique is applied here to one sample per stratigraphic unit, as previously performed by Balescu et al. (2003, 2010), Timar et al. (2010), Timar-Gabor et al. (2011) and Vasilinuic et al. (2012, 2013) when testing their luminescence dating techniques on the Middle Pleistocene Romanian loess (L2, L3). This sampling strategy aims at obtaining the mean depositional age of each loess layer to validate the MS age model of Jordanova et al. (2008).

3. Methods

3.1. Sample preparation, equivalent dose (D_e) determination and fading corrections

All dated samples were collected from homogeneous, unweathered and unreworked loess. In addition to field observations, sample positions within each loess horizon have been chosen on the basis of the field MS variations, measured by field kappa meter KT-5 (SatisGeo s.r.o., Czech Republic).

The IRSL samples were wet sieved and subsequently treated with HCl (10%) to remove calcium carbonate.

All IRSL measurements were performed on K-feldspar fine sand-size grains (60-80 µm). K-feldspars (density < 2.58 g/cm^3.) were separated using a heavy solution of sodium polytungstate. The mineral grains were dispensed on aluminium disks or aluminium cups.

For the D_e determinations, two protocols were used (Table S3): the SAR pIRIR$_{290}$ technique on single aliquots (monolayer of grains on disk; sample diameter of 4 mm) and the multiple-aliquot additive-γ dose (MAAD IRSL$_{50}$) protocol (20 mg of grains in cups, 20 aliquots).

In the SAR pIRIR$_{290}$ protocol, single aliquots are exposed to increasing regenerated dose. Interpolation of the natural signal on the dose response curve yields the D_e (Fig. 3). In the standard MAAD protocol (Aitken, 1998; Singhvi et al., 1982), a series of increasing doses are added to the natural sample, and the resultant dose response is extrapolated back to a negligible light level to obtain the D_e (Fig. 4). The advantage of this protocol over SAR pIRIR is that sensitivity changes are kept to a minimum and sensitivity corrections are therefore not usually used.

This technique has recently been successfully re-explored in the context of the violet stimulated luminescence signal of quartz from the Chinese loess (Ankjaegaard et al., 2016).

The MAAD protocol remains valid for well-bleached sediments such as loess whose wind-blown nature ensures that their luminescence clock was completely reset prior to deposition. Moreover, it should be noted that the MAAD protocol has previously been shown to provide a good chronological discrimination between the MIS 8, MIS 6 and MIS 2-4 loess deposits of SE Romania (Balescu et al., 2003, 2010) thereby providing a reliable and very useful chronostratigraphic marker. In the present study, the MAAD approach applied in conjunction with the $pIRIR_{290}$ technique, is aimed at obtaining an additional age control. It also allows direct comparison with the MAAD $IRSL_{50}$ ages previously obtained for the three upper loess layers (L1-L3) in SE Romania (at Tuzla, Mircea Vodă and Mostistea) (Balescu et al., 2003, 2010).

The $pIRIR_{290}$ and MAAD $IRSL_{50}$ measurements were performed respectively on a Lexsyg Smart reader and an automated Daybreak 1100TL reader. Aliquots measured on the Lexsyg Smart reader were irradiated with the internal ^{90}Sr /^{90}Y beta source (0.13 Gy/s). Those measured on the Daybreak systems were irradiated with an external ^{137}Cs gamma source (0.03 Gy/s). The luminescence of K-feldspars was detected with a 410 nm detection window (combination of Schott BG39 glass and Semrock 414/46 Brightline HC interference filters) on the Lexsyg Smart reader and through a blue-violet filter combination (Corning 7-59 and Schott BG39) on the Daybreak systems. The growth curves of the K-feldspar samples were fitted with a single saturating exponential function. The signal used for analysis was obtained from the net initial signal (5 s), subtracted by the background signal taken at the end of the IRSL decay (last 20 s). The Central Age Model (Galbraith et al., 1999) was used for the mean D_e calculation.

All samples behave well in the $pIRIR_{290}$ protocol (in terms of recycling, recuperation and dose recovery). Recuperation level was very low, being on average close to 0.47 %, and all less than 1 %. The recycling ratios of all samples range from 0.98 to 1.01, for an average of 1.00 ± 0.01. The recycled dose point (last versus first) was chosen to be half of the equivalent dose. A dose recovery test was conducted on K-feldspars from sample KA 2. These were bleached 1h with an external solar simulator (Honlë SOL2) and given a dose of 500 Gy. We measured a recovered to given dose ratio of 1.05 ± 0.03 (n=3).

In our $pIRIR_{290}$ protocol, we used a test dose of 133 Gy. Colarossi et al. (2018) have recently shown that the magnitude of the luminescence response (Tx) to the test dose is dependent upon the size of the luminescence signal (Lx) arising from the regeneration dose when using the $pIRIR_{225}$ protocol on single grain (IRSL at 225°C for 2 s). They have demonstrated that when the test dose is small (1-15% of the given dose) the carry-over of charge dominates the signal

arising from the test dose, whereas for larger test doses this impact is much lower. It should be stressed however that in the present study, our $pIRIR_{290}$ protocol has been validated by a recovery dose test. Also, we used a large test dose, between 15-80% of the De, as recommended by Yi et al. (2016) who have shown that in this dose range, large given doses were successfully recovered. But since we are using a higher stimulation temperature (290°C) and a longer stimulation time (200 sec), our results cannot be directly compared with those of Colarossi et al. (2018). Nevertheless, future application of the modified protocol of Colarossi et al. (2018) designed to minimize the impact of the regeneration dose upon the measurement of the test dose, might be useful to corroborate our results.

The K-feldspar $IRSL_{50}$ signal being affected by anomalous fading (i.e. an unexpected loss of signal through time leading to an age underestimation), all our measured MAAD $IRSL_{50}$ ages have been corrected for fading using the protocol of Mejdahl (1988, 1989) as previously described in Balescu et al. (2003, 2010) (see Supplementary information). It relies on the IRSL analysis of "infinitely old" K-feldspars, here collected from L7 at Viatovo (VIA 7), below the MBB. All MAAD measurements have been performed on K-feldspar samples that have been stored 1 year at room temperature after irradiation in order to reduce the effect of anomalous fading (Spooner, 1992).

By contrast, the $pIRIR_{290}$ signal of the Bulgarian loess shows extremely low fading rates suggesting in this case, that this is a stable, non-fading signal. Anomalous fading rates (g-value) were measured using the SAR protocol of Auclair et al. (2003). Fading measurements were carried out on about 12 aliquots per sample (Table S4). All loess layers show similar and extremely low fading rates (g-values); the mean g-value ranging between -0.04 and 0.18 %/decade. Consequently, in the present study, the $pIRIR_{290}$ ages have not been corrected for fading. It should be stressed that similar low and negative fading rates were also observed in the NW Bulgarian loess of Harletz (Lomax et al., 2018) and in the Romanian loess (Vasiliniuc et al., 2012) and have been assumed by these authors to be a laboratory artefact.

3.2. Dose rate determination

The concentrations of U, Th and K were measured through gamma spectrometry. For the conversion to dose rate we used the absorbed beta dose coefficient given in Nathan (2010) while we relied on Brennan et al. (1991) for the alpha absorption coefficient. The past water content was estimated at 20 ± 5% (the average of the present-day natural water content and the laboratory saturated water content). The cosmic dose rates were estimated using the present-day burial depth of the sample (Prescott and Hutton, 1994). The dose rates were calculated using the DRAC (Durcan et al., 2015). As suggested by Huntley and Baril (1997) we assumed

an internal K content of 12.5 ± 0.5% for the blue IRSL emission of the K-feldspars. The summary of the dose rates is reported in Table S5.

4. Results and discussion

4.1. Dose rates and luminescence age estimates of the NE Bulgarian loess

All loess layers display similar dose rates, ranging between 2.94 and 3.43 Gy/ka (Table S6), except in the case of sample KA 1 collected within the loess L1 at Kaolinovo. This sample KA 1 with a much higher dose rate of 5.13 Gy/ka due to higher radionuclide concentrations, yielded a $pIRIR_{290}$ age of 45 ± 2 ka (Table 1). This higher dose rate could possibly be related to the presence of a tephra layer equivalent to the Campanian Ignimbrite/Y5 (39.28 ± 0.11 ka) reported at Rasova-Valea cu Pietre in SE Romania (Fig. 1B). Anechitei-Deacu et al. (2013) have shown that loess samples collected at that site, in L1 around this ash layer exhibited a similar radionuclide enrichment. This tephra layer has also been identified within L1 at Caciulatesti (Southern Romania; Constantin et al., 2012) and at Urluia (Dobrogea; Fitzsimmons and Hambach, 2014) (Fig. 1B). This is clearly a matter that requires further investigation.

Comparative dose response curves of the $pIRIR_{290}$ signal are shown in Figure 3. Representative $IRSL_{50}$ additive growth curves are presented in Figure 4. The luminescence results for the NE Bulgarian loess are reported in Table 1. The $pIRIR_{290}$ ages and the fading corrected MAAD-$IRSL_{50}$ ages are self-consistent within the error limits, and both show stratigraphic consistency.

- For L1, these luminescence ages range between 41 and 69 ka and for L2 between 153 and 213 ka. These results demonstrate for the first time that the two uppermost loess units, L1 and L2, at Viatovo and Kaolinovo, were deposited respectively during MIS 2-4 and MIS 6, thereby confirming the expected burial age previously inferred from the magnetostratigraphy age model established by Jordanova et al. (2008).
- For L3, the $pIRIR_{290}$ ages (293 ± 17 and 296 ± 17 ka) suggest a MIS 8 age. They should be considered as minimum ages since the natural ratios (Ln/Tn) of L3 are close to the laboratory saturation level of the growth curve (Fig. 3). Their measured D_e values are systematically higher than $2D_0$ (Table 1). The correlation of L3 with MIS 8 is also supported by the corrected MAAD-$IRSL_{50}$ ages of L3 (285 ± 35 ka; 264 ± 64 ka) whose corrected D_e values are lower than $2D_0$ (Table 1).
- The natural $pIRIR_{290}$ signal of the infinitely old sample VIA 7 (L7) is in saturation as expected for a non-fading signal (Fig. 3). Whereas the natural MAAD $IRSL_{50}$ signal of this infinitely old sample VIA 7 (L7) is not in saturation (Fig. 4) due to fading in the

environment (Mejdahl, 1988). It yields an apparent IRSL age of 296 ± 60 ka in good agreement with the apparent IRSL age of L7 at Tuzla in SE Romania (271 ± 39 ka; Balescu et al., 2003). The measured D_e value of VIA 7 (L7) is lower than $2D_0$ (Table 1). It is worth pointing out that infinitely old loess, lying below the MB boundary, in Romania, Bulgaria, Serbia and Hungary yield similar apparent ages, suggesting an upper age limit of around 250-300 ka, when using either the $IRSL_{50}$ or the pIRIR protocols: 271 ± 39 ka ($IRSL_{50}$) at Tuzla in Romania (Balescu et al., 2003), 296 ± 60 ka ($IRSL_{50}$) and >250 ka ($pIRIR_{290}$) at Viatovo in Bulgaria (this study), 239 ± 38 ka ($IRSL_{50}$) and >260 ka ($pIRIR_{290}$) at Stari Slankamen in Serbia (Murray et al., 2014), 316 ± 36 ka ($IRSL_{50}$) at Paks in Hungary (Frechen et al., 1997).

These luminescence ages may further be compared with those recently obtained for the Harletz loess sequence in NW Bulgaria (Fig. 1B). This sequence consists of three loess layers separated by two palaeosol complex (Lomax et al., 2018). The oldest loess unit rests on alluvial deposits of the Ogosta river (tributary of the Danube). Luminescence dating was carried out using the quartz fine grain fraction and a SAR protocol, and the feldspar coarser grain fraction (63-125 µm), applying the MET-pIRIR protocol. The OSL and MET-pIRIR ages of the youngest loess unit (L1: 36-67 ka) are in good agreement with those obtained for L1 at Viatovo and Kaolinovo (Table S6). The underlying loess unit (L2) yielded underestimated OSL ages (84-110 ka). Whereas the MET-pIRIR ages of L2, ranging between 131 and 185 ka are in good accordance with those of L2 at Viatovo and Kaolinovo (Table S6). By contrast, the oldest loess unit, resting on alluvial sediments and overlain by an interglacial paleosol supposedly assigned to MIS 7, yielded an underestimated MET-pIRIR age of 131 ± 10 ka.

4.2. Comparison of the NE Bulgarian and SE Romanian loess-paleosol sequences

The NE Bulgarian and SE Romanian loess deposits belong to the same lower Danube loess area. They exhibit common characteristics and cover the same age range. In both regions, the MBB has been identified in the oldest loess L7 (Jordanova et al., 2008; Balescu et al., 2003). Moreover, the luminescence chronology of the three upper loess units (L1-L3) in SE Romania is now securely established thanks to the application of multiple dating protocols. Hence, it is worth comparing here their luminescence chronologies, along with their pedostratigraphic and magnetostratigraphic records.

337 *4.2.1. Luminescence chronologies*

338

339 So far, four different luminescence dating techniques have been applied to the SE Romanian
340 loess: the MAAD-$IRSL_{50}$ on K-feldspar silt-size grains (Balescu et al., 2003, 2010), the OSL on
341 fine and coarse quartz grains (Timar et al., 2010; Timar-Gabor et al., 2011; Vasiliniuc et al,
342 2011; Constantin et al., 2012, 2014, 2015; Anechitei-Deacu et al., 2013; Timar-Gabor and
343 Wintle, 2013; Fitzsimmons and Hambach, 2014) and more recently, the SAR $IRSL_{50}$
344 (Vasiliniuc et al., 2013) and the $pIRIR_{225}$ on polymineral fine grains (Vasiliniuc et al., 2012).
345 These dating techniques have been tested on several long loess sequences showing a similar
346 superposition of loess and interbedded paleosols: at Tuzla (Balescu et al., 2003, 2010),
347 Costineşti (Timar-Gabor and Wintle, 2013; Constantin et al., 2014), Mircea Vodă (Balescu et
348 al., 2010; Timar et al., 2010; Timar-Gabor et al., 2011; Vasiliniuc et al., 2012), Urluia
349 (Fitzsimmons et al., 2013; Fitzsimmons and Hambach, 2014), Mostiştea (Balescu et al., 2010;
350 Vasiliniuc et al., 2011) and Lunca (Constantin et al., 2015) (Fig. 1B). It is also worth pointing
351 out that the accuracy of the quartz OSL dating technique has been demonstrated on loess
352 samples bracketing a well-dated volcanic tephra layer (Campanian Ignimbrite/Y5:
353 39.28 ± 0.11 ka) within the Last Glacial (L1) loess, at Urluia (Fitzsimmons and Hambach,
354 2014), Caciulateşti (Constantin et al., 2012), and Rasova-Valea cu Pietre (Anechitei-Deacu et
355 al., 2013; Zeeden et al., 2018) (Fig. 1B).
356 For the sake of comparison with the NE Bulgarian loess, we will focus here on the three most
357 investigated and better documented long loess sections from SE Romania (Tuzla, Mircea Vodă
358 and Mostiştea) where both the Upper and Middle Pleistocene loess deposits (L1, L2, L3), lying
359 in stratigraphic continuity, have previously been dated using multiple luminescence dating
360 protocols.
361 The Tuzla section is a cliff-exposure along the Black Sea shore comprising seven loess layers
362 (L1-L7) and six intercalated paleosols (S1-S6) (Fig. 2, Fig. S3). It is the longest loess sequence
363 in Romania spanning the last 800 ka. The Brunhes-Matuyama geomagnetic reversal has been
364 identified by J. Hus in loess L7 (Balescu et al., 2003). The Mircea Vodă section located on the
365 Dobrogea plateau and the Mostiştea section lying in the southern Danube plain show a
366 superposition of six (L1-L6) and four (L1-L4) loess layers, respectively (Fig. 2). Their
367 stratigraphy is reported on Figure 2. The comparative luminescence ages obtained for the three
368 uppermost loess units (L1, L2, L3) in NE Bulgaria and SE Romania are summarized in Table
369 S6. It should be pointed out that at Mircea Vodă and Mostiştea, a high-resolution sampling has
370 been performed within the upper loess layer L1 (Timar et al., 2010; Timar-Gabor et al., 2011;

371 Vasilinuic et al., 2012, 2013) in order to estimate the depositional age range and loess
372 accumulation rate.
373 As shown in Table S6, the OSL ages on fine quartz grains (4-11 μm) at Mircea Vodă provided
374 accurate ages for the Last Glacial loess (L1 unit) but they severely underestimated the expected
375 burial ages below the S1 paleosol (Timar et al., 2010; Timar-Gabor et al., 2011; Vasiliniuc et al
376 2011). The OSL ages on coarser quartz grains (63-90 μm), at Mostiştea, Mircea Vodă and
377 Costineşti, are systematically higher than those obtained from fine quartz grains, both in L1 and
378 L2. The cause for this age discrepancy still remains under investigation; the differences
379 between the natural and the laboratory dose response for the two quartz fractions are believed
380 to be a cause for the observed age discrepancy (Timar-Gabor and Wintle, 2013; Constantin et
381 al., 2014, 2015).
382 At Mircea Vodă, Vasiliniuc et al. (2013) applied the SAR $IRSL_{50}$ technique to polymineral fine
383 grains (4-11 μm) from loess L1 to L4 but their SAR $IRSL_{50}$ ages have a questionable accuracy
384 due to the poor dose recovery performances. These polymineral fine grain samples (from L1 to
385 L4) have also been dated using the $pIRIR_{225}$ technique (Vasiliniuc et al., 2012). Their fading
386 rate values are all close to 1 %/decade and assumed to be a laboratory artefact. Therefore,
387 Vasiliniuc et al. (2012) choose not to correct their $pIRIR_{225}$ ages for fading. For L1, they
388 measured $pIRIR_{225}$ ages ranging from 70 ± 11 ka to 19 ± 3 ka, up-section. For L2 and L3 and
389 L4, they obtained $pIRIR_{225}$ ages of respectively, 138 ± 22 ka, 245 ± 42 ka and 360 ± 71 ka,
390 consistent with the expected geological ages. However, the $pIRIR_{225}$ ages of L3 and L4 are
391 only minimum ages since the natural $pIRIR_{225}$ signals of L3 and L4 are respectively, close to
392 saturation and in saturation. The $pIRIR_{225}$ technique is therefore restricted at Mircea Vodă to
393 the three last glaciations. This is consistent with the behaviour that has been observed for L3 in
394 NE Bulgaria. This contrasts with the natural $IRSL_{50}$ signals of both the polymineral fine grains
395 (Vasiliniuc et al., 2012, 2013) and the K-feldspar silt grains (Balescu et al., 2003, 2010) of the
396 loess L3 in SE Romania and NE Bulgaria which have a much later saturation (higher D_0
397 values), thus opening the way for dating loess older than L3 (MIS 8). This is the object of
398 further investigation.
399 As shown in Table S6, the MAAD $IRSL_{50}$ and $pIRIR_{290}$ ages of the Middle Pleistocene
400 NE Bulgarian loess (L2, L3) are consistent with the MAAD-$IRSL_{50}$ and $pIRIR_{225}$ ages obtained
401 in SE Romania. For the Last Glacial loess L1, in SE Romania and NE Bulgaria, there is a good
402 agreement among the feldspar luminescence ages obtained using multiple techniques (SAR
403 $IRSL_{50}$, MAAD $IRSL_{50}$, $pIRIR_{225, 290}$ and MET-pIRIR). They range from 70 ± 11 ka to 19 ± 3
404 ka, covering the MIS 4-2 time interval.
405

406
407 *4.2.2. Pedostratigraphic records*
408
409 The pedostratigraphic records of the Viatovo and Kaolinovo loess sequences (Fig. 2) lying in
410 the Ludogorie region show the same gradual transition to increasingly cooler and drier
411 interglacial climate conditions, up-section from S6 to S0. At both sites, the red paleosols (forest
412 soils) preserved in the lower part of the loess sequences (S4-S6) are overlain by chernozem-like
413 paleosols (S0-S3) developed in drier climatic conditions (steppic soils). This succession of soils
414 reflects a regional trend of increased aridification in interglacial climate during the Middle
415 Pleistocene (Jordanova et al., 2008). A similar climatic trend was observed at Koriten in the
416 Bulgarian Dobrogea (Jordanova and Petersen, 1999a,b) and in SE Romania (Tuzla, Mircea
417 Vodă , Mostiştea) (Conea, 1969; Panaiotu et al., 2001; Buggle et al., 2009; Balescu et al., 2010;
418 Fitzsimmons et al., 2012; Marković et al., 2015). However, at Koriten and in SE Romania
419 (Tuzla, Mircea Vodă, Mostiştea) (Fig. 2), the lower rubified interglacial soils (S3-S6) are
420 overlain by steppe-forest soils (brown red soils; S1-S2) instead of Chernozems. This might
421 suggest a shift towards drier climatic conditions westwards (in the Ludogorie region) during
422 MIS 7 and MIS 5. It is worth also to emphasize that the transition from warm and humid
423 towards cooler and drier climatic conditions occurred at Viatovo and Kaolinovo during MIS 9
424 with the first chernozem-like paleosol (S3), whereas further east, at Koriten and in SE Romania
425 (Tuzla, Mircea Vodă, Mostiştea), it occurred during MIS 7 with the first steppe-forest soil (S2)
426 (Fig. 2).
427
428 *4.2.3. Magnetostratigraphic records*
429
430 At Koriten and Viatovo, the magnetostratigraphic characterization of the loess-paleosol
431 sequences provided the first chronostratigraphic framework for the Bulgarian loess (Jordanova
432 and Petersen, 1999; Jordanova et al., 2007, 2008). The magnetic susceptibility (MS) of the
433 loess-paleosol sequences has been widely used for interregional correlations of Pleistocene
434 loess across the lower and middle Danube basin and has also been proved to be a valuable
435 proxy for the reconstruction of past climate changes in this area during the Middle and Upper
436 Pleistocene (Jordanova and Petersen, 1999a,b; Panaiotu et al., 2001; Jordanova et al., 2007,
437 2008; Hambach et al., 2008; Buggle et al., 2008, 2009; Marković et al., 2011, 2015;
438 Fitzsimmons et al., 2012; Zeeden et al., 2016). Paleosols are identifiable by a characteristic
439 increase in MS value; this enhancement with strongly magnetic minerals is related to
440 pedogenesis. Hence, the MS variations clearly reflect here the pedostratigraphy of the loess-
441 paleosol sequences.

On Figure 5, the MS record of the new Kaolinovo loess sequence (unpublished data) is compared to the previously published MS records of Koriten, Mostiştea and Mircea Vodă. As shown on this figure, the loess-paleosol sequences from Koriten and SE Romania, lying eastwards in the Dobrogea area and in the southern Romanian Danube Plain, exhibit the same MS signatures. They register higher MS values in the older red paleosols (S3-S6) and lower MS values in the upper forest-steppe soils (S1, S2). Interestingly, the first stratigraphic correlation between the Romanian and Bulgarian loess sequences established by Panaiotu et al. (2001) relied on the similarity of the Mostiştea and Koriten MS records.

By contrast the Viatovo and Kaolinovo loess-paleosol sequences, lying westwards in the Ludogorie region, show different MS records. At Viatovo, the MS values of the younger chernozem-like paleosols (S1-S3), formed in an arid context are comparatively higher than those of the older red paleosols (S4-S6) developed under forest vegetation and more humid conditions (Hanesch and Scholger, 2005; Jordanova et al., 2016). This could be ascribed to the predominance of strongly magnetic maghemite pedogenic minerals in the chernozem-like soils and the smaller contribution of weakly magnetic hematite (Jordanova et al., 1997). While in the older red paleosols a significant part of the pedogenic fraction is represented by hematite resulting in a lower magnetic susceptibility enhancement. Also, the Kaolinovo MS record exhibits a more variable picture. The S3 paleosol presents a lower magnetic susceptibility enhancement as compared to the signal of the two younger paleosols (S2 and S1). This difference is most probably a result of subsequent water logging conditions which would have partially dissolved the finest pedogenic strongly magnetic iron oxides and established the observed redoximorphic features.

The cause for this spatial variability in MS signatures among the Bulgarian loess palaeosol sequences and the full palaeoclimatic implications of these MS results will be the subject of another study.

5. Conclusions

This study is the first attempt to assess the luminescence ages to the key reference loess-paleosol sequence of Viatovo in NE Bulgaria. It appears to provide a reliable chronological framework for the Bulgarian loess over the last 300 ka.

The MAAD $IRSL_{50}$ and $pIRIR_{290}$ ages measured on K-feldspars from L1, L2 and L3 at Viatovo and Kaolinovo (NE Bulgaria) are in good agreement with the burial ages expected from stratigraphic and magnetostratigraphic evidence. Hence, it validates the chronostratigraphic framework suggested by Jordanova et al. (2008) on the basis of the MS signature of the loess-

paleosol sequence. Moreover, the luminescence ages of the NE Bulgarian loess (L1-L3) are in good accordance with both the MAAD $IRSL_{50}$ and the $pIRIR_{225}$ ages of the three uppermost loess layers (L1-L3) from SE Romania. This IRSL investigation therefore provides new perspectives for confident interregional correlations of Pleistocene loess across the lower Danube basin.

The SE Romanian and NE Bulgarian loess-paleosol sequences record valuable pedostratigraphic and magnetic susceptibility data, which in the light of these new luminescence dates, should provide further insights into the palaeoclimatic evolution of the lower Danube basin during the Middle Pleistocene.

The pedostratigraphic records of the SE Romanian and NE Bulgarian loess-paleosol sequences indicate similar palaeoclimatic trends with progressive aridification during interglacials. However the transition from humid and warm to cooler and drier interglacial conditions occurred much earlier westwards, in the Ludogorie area (paleosol S3, MIS 9), than in the Dobrogea area (paleosol S2, MIS 7).

Acknowledgement

The authors would like to thank Michelle Laithier (UQAM, Montréal) and Floriane Peudon (Université de Lille) for preparing the illustrations. We would also like to express our gratitude to both anonymous reviewers for their constructive comments which improved an earlier version of the manuscript.

References

1- Aitken, M.J., 1998. An introduction to Optical Dating: The Dating of Quaternary Sediments by the Use of Photon-stimulated Luminescence. Oxford University Press, Oxford: New York. 280p.

2- Anechitei-Deacu, V., Timar-Gabor, A., Fitzsimmons, K.E., Veres, D., Hambach, U., 2013. Multi-method luminescence investigations on quartz grains of different sizes extracted from a loess section in southeast Romania interbedding the Campanian Ignimbrite ash layer. Geochronometrica 41 (1), 1-14.

3- Ankjaergaard, C., Guralnik, B., Buylaert, J.-P., Reimann, T., Yi, S.W., Wallinga, J., 2016. Violet stimulated luminescence dating of quartz from Luochan (Chinese loess plateau): Agreement with independent chronology up to ~ 600 ka. Quaternary Geochronology 34, 33-46;

4- Auclair, M., Lamothe, M, Huot, S., 2003. Measurement of anomalous fading for feldspar IRSL using SAR. Radiation Measurements 37, 487-492.

5- Balescu, S., Lamothe, M., Mercier, N., Huot, S., Balteanu, D., Billard, A., Hus J, 2003. Luminescence chronology of Pleistocene lœss deposits from Romania: testing methods of age correction for anomalous fading in alkali feldspars. Quaternary Science Reviews 22, 967-973.

6- Balescu, S., Lamothe, M., Panaiotu, C.G., Panaiotu, C.E., 2010. La chronologie IRSL des séquences loessiques de l'Est de la Roumanie. Quaternaire 21 (2), 115-126.

7- Brennan, B.J., Lyons, R.G., Phillips, S.W., 1991. Attenuation of alpha particle track dose for spherical grains. Nuclear Tracks and Radiation Measurements 18, 249-253.

8- Buggle, B., Glaser, B., Zöller, L., Hambach, U., Markovic, S., Glaser, I., Gerasimenko, N., 2008**.** Geochemical characterization and origin of Southeastern and Eastern lœsses (Serbia, Romania, Ukraine). Quaternary Science Reviews 27**,** 1058-1075.

9- Buggle, B., Hambach, U., Glaser, B., Gerasimenko, N., Marković, S., Glaser, I., Zöller, L., 2009, Stratigraphy, and spatial and temporal paleoclimatic trends in Southeastern/Eastern loess-paleosol sequences.Quaternary International 196, 86-106.

10- Buylaert, J.-P., Jain, M., Murray, A.S., Thomsen, K., Thiel, C., Sohbati, R., 2012. A robust feldspar luminescence dating method for Middle and Late Pleistocene sediments. Boreas 41, 435-451.

11- Conea, A., 1969**.** Profils de lœss en Roumanie. *In* J. Fink (ed.), La stratigraphie des lœss d'Europe. Supplément du Bulletin de l'Association Française pour l'Etude du Quaternaire, INQUA, 127-134.

12- Constantin, D., Timar-Gabor, A., Veres, D., Begy, R., Cosma, C. 2012. SAR-OSL dating of different grain-sized quartz from a sedimentary section in southern Romania interbedding the Campanian Ignimbrite/Y5 ash layer. Quaternary Geochronology 10, 81-86.

13- Constantin, D., Begy, R., Vasiliniuc, S., Panaiotu, C., Necula, C., Codrea, V., Timar-Gabor, A., 2014. High-resolution OSL dating of the Costinesti section (Dobrogea, SE Romania) using fine and coarse quartz. Quaternary International 334-335, 20-29.

14- Constantin, D., Cameniţă, A., Panaiotu, C., Necula, C., Codrea, V., Timar-Gabor, A., 2015. Fine and coarse-quartz SAR-OSL dating of Last Glacial loess in Southern Romania. Quaternary International 357, 33-43.

15- Colarossi, D., Duller, G.A.T., Roberts, H.M., 2018. Exploring the behaviour of luminescence signals from feldspars: Implications for the single aliquot regenerative dose protocol. Radiation Measurements, 109, 35-44.

16- Durcan, J. A., King, G. E., Duller G.A.T., 2015. DRAC: Dose Rate and Age Calculator for trapped charge dating. Quaternary Geochronology 28, 54-61.

17- Eckmeier, E., Gerlach, R., Gehrt, E., Schmidt, M.W.I., 2007. Pedogenesis of Chernozems in Central Europe - A review. Geoderma 139, 288-299.

18- Evlogiev, J., 2007. Evidence for the Aeolian Origin of Loess in the Danubian Plain. Geologica Balkanica, 36 (3-4), 31-39.

19- Fitzsimmons, K. E., Marković, S. B., Hambach, U., 2012. Pleistocene environmental dynamics recorded in the loess of the middle and lower Danube basin. Quaternary Science Reviews 41, 104-118.

20- Fitzsimmons, K.E., Hambach, U., Veres, D., Iovita R., 2013. The Campanian Ignimbrite eruption: new data on volcanic ash dispersal and its potential impact on human evolution; PLoS One 8/6, e65839.

21- Fitzsimmons, K. E. Hambach, U., 2014. Loess accumulation during the last glacial maximum: evidence from Urluia, southeastern Romania. Quaternary International 334-335, 74-85.

22- Fotakieva, E., 1974. The first fossil soil (Wurmian interstadial) in the loess of Northern Bulgaria. Soil Science and Agrochemistry IX (5), 3-10 (in Bulgarian, with English abstract).

23- Frechen, M., Horvath, E., Gabris, G. 1997. Geochronology of Middle and Upper Pleistocene loess sections in Hungary. Quaternary Research, 48, 291-312.

24- Galbraith, R. F., Roberts, R.G., Laslett, G.M., Yoshida, H., Olley, J.M, 1999. Optical dating of single and multiple grains of quartz from Jinmium Rock Shelter, Northern Australia: Part I, Experimental Design and Statistical Model. Archaeometry 41, 339-364.

25- Haase, D., Fink, J., Haase, G., Ruske, R., Pécsi, M., Richter, H., Altermann, M., Jäger, K.D., 2007. Loess in Europe - its spatial distribution based on a European Loess Map, scale 1:2,500, 000. Quaternary Science Reviews 26, 1301-1312.

572 26- Hambach, U, Rolf, C., Schnepp, E., 2008. Magnetic dating of Quaternary sediments,
573 volcanites and archaeological materials: an overview. Eiszelalter und Gegenwart;
574 Quaternary Science Journal 57, 25-51.
575 27- Hanesh, M., Scholger, R., 2005. Lithological and pedological influences on the magnetic
576 susceptibility measured throughout soil profiles. Geophysical Journal International 161 (1),
577 50-56.
578 28- Huntley, D.J., Baril, M.R., 1997. The K content of the K-feldspars being measured in
579 optical dating or in thermoluminescence dating. Ancient TL 15, 11-13.
580 29- Jipa, D. C., 2014. The loess-like deposits in the Lower Danube basin. Genetic significance.
581 Geo-Eco-Marina, 20, 7-18.
582 30- Jordanova, D., Petrovsky, E., Jordanova, N., Evlogiev J., Butchvarova, V., 1997.
583 Rockmagnetic properties of recent soils from North Eastern Bulgaria. Geophysical Journal
584 International 128, 474-488.
585 31- Jordanova, D., N. Petersen, 1999a. Palaeoclimatic record from loess-soil section in NE
586 Bulgaria. Part I: Rock-magnetic properties. Geophysical Journal International 138, 520-532.
587 32- Jordanova, D., Petersen, N., 1999b. Paleoclimatic record from lœss-soil profile in
588 northeastern Bulgaria – Part II: Correlation with global climatic events during the
589 Pleistocene. Geophysical Journal International 138, 533-540.
590 33- Jordanova, D., Hus, J., Geeraerts, R., 2007. Palaeoclimatic implications of the magnetic
591 record from loess/palaeosol sequence Viatovo (NE Bulgaria). Geophysical Journal
592 International 171, 1036-1047
593 34- Jordanova, D., Hus, J., Evlogiev, J., Geeraerts, R., 2008. Palaeomagnetism of the
594 lœss/palaeosol sequence in Viatovo (NE Bulgaria) in the Danube basin. Physics of the Earth
595 and Planetary Interiors 167, 71-83.
596 35- Jordanova N., Jordanova D., Petrov P., 2016. Soil magnetic properties in Bulgaria at a
597 national scale - Challenges and benefits. Global and Planetary Change 137, 107-122.
598 36- Kis, E., Schweitzer, F., Palcsu, L., Futo, I., Balogh, J., Di Gléria, M., 2012. Investigations
599 of paleogeographic variations on the basis of the stratotype section of Viatovo at the Lower
600 Danube. Hungarian Geographical Bulletin 61 (2), 93-111.
601 37- Lomax, J., Fuchs, M., Antoine, P., Rousseau, D.-D., Lagroix, F., Hatté, C., Taylor, S.N.,
602 Till, J.L., Debret, M., Moine, O., Jordanova, D., 2018. Luminescence chronology of the
603 Harletz loess sequence, Bulgaria. Boreas, 48 (1), 179-194.
604 38- Marković, S. B., Hambach, U., Stevens, T., Kukla, G., Heller, F., McCoy, W.D., Oches,
605 E.A., Buggle, B., Zöller, L., 2011. The last million years recorded at the Stari Slankamen
606 (Northern Serbia) loess-palaeosol sequence: revised chronostratigraphy and long-term
607 environmental trends. Quaternary Science Reviews 30, 1142-1154.
608 39- Marković, S. B., Stevens, T., Kukla, G., Hambach, U., Fitzsimmons, K., Gibbard, P.,
609 Buggle, B., Zech, M., Guo, Z., Hao, Q., Wu, H., O'Hara Dhand, K., Smalley, I., Újvári, G.,
610 Sümegi, P., Timar-Gabor, A., Veres, D., Sirocko, F., Vasiljević, D.A., Jary, Z., Svensson,
611 A., Jović, V., Lehmkuhl, F., Kovács, J., Svirčev, Z., 2015. Danube loess stratigraphy -
612 Towards a pan-European loess stratigraphic model. Earth-Science Reviews 148, 228-258.
613 40- Mejdahl, V., 1988. Long-term stability of the TL signal in alkali feldspars. Quaternary
614 Science Reviews 7, 357-360.
615 41- Mejdahl, V., 1989. How far back: life times estimated from studies of feldspars of infinite
616 ages. *In* M.J. Aitken (ed.), Synopses from a Workshop on "Long and Short Range Limits in
617 Luminescence Dating". Occasional Publication 9, The Research Laboratory for Archaeology
618 and the History of Art, Oxford University, Oxford, 53-58.
619 42- Minkov, M., 1968. Loess in North Bulgaria. Bulgarian Academy of Sciences, Sofia (in
620 Bulgarian).
621 43 Nathan, R.P., 2010. Numerical modelling of environmental dose rate and its application to
622 trapped-charge dating. Ph.D thesis, University of Oxford.

44- Murray, A., Schmidt, E., Stevens, T., Buylaert, J.-P., Marković, S., Tsukamoto, S., Frechen, M., 2014. Dating Middle Pleistocene loess from Stari Slankamen (Vojvodina, Serbia) - Limitations imposed by the saturation behaviour of an elevated temperature IRSL signal. Catena 117, 34-42.

45- Panaiotu, C.G., Panaiotu, E.C., Grama, A., Necula, C., 2001. Paleoclimatic Record from a Lœss-Paleosol Profile in Southeastern Romania. Physics and Chemistry of the Earth (A) 26, 893-898.

46- Prescott, J.R., Hutton, J.T., 1994. Cosmic ray contributions to dose rates for luminescence and ESR dating: Large depths and long-term time variations. Radiation Measurements 23, 497-500.

47- Radan, S. C., 2012. Towards a synopsis of dating the loess from the Romanian Plain and Dobrogea: authors and methods through time. Geo-Eco-Marina 18/2012, 153-172.

48- Shackleton, N., Berger, A., Peltier, R., 1990. An alternative astronomical calibration of the lower Pleistocene time scale based on ODP site 677. Trans. Royal Soc. Edimburg Earth Sci. 81 251-261.

49- Singhvi, A.K., Sharma, Y.P., Agrawal, D.P., 1982. Thermoluminescence dating of dune sands in Rajasthan, India. Nature 295, 313-315.

50- Smalley, I., Leach, 1978. The origin and distribution of the loess in the Danube basin and associated regions of East - Central Europe - a review. Sedimentary Geology 21, 1-26.

51- Smalley, I. Ken O'Hara-Dhanda, Wint, J., Machalett, B., Jary, Z., Jefferson, J., 2009. Rivers and loess: The significance of long river transportation in the complex event-sequence approach to loess deposit formation. Quaternary International 198, 7-18.

52- Spooner, N. A., 1992. Optical dating: preliminary results on the anomalous fading of luminescence from feldspars. Quaternary Science Reviews 11, 139-145.

53- Stuut, J.-B., Smalley, I., O'Hara-Dhand, K., 2009. Aeolian dust in Europe: African sources and European deposts. Quaternary International 198, 234-245.

54- Suganuma, Y., Okada, M., Horie, K., Kaiden, H., Takehara, M., Senda, R., Kimura, J.-I., Kawamura, K., Haneda, Y., Kazaoka, O., Head, M.J., 2015. Age of Matuyama-Brunhes boundary constrained by U-Pb zircon dating of a widespread tephra. Geology 43(6), 491-494.

55- Thomsen, K.J., Murray, A.S., Jain, M., Botter-Jensen, L., 2008. Laboratory fading rates of various luminescence signals from feldspar-rich sediment extracts. Radiation Measurements 43, 1474-1486.

56- Timar-Gabor, A., Wintle, A.G. 2013. On natural and laboratory generated dose response curves for quartz of different grain sizes from Romanian loess. Quaternary Geochronology 18, 34-40.

57- Timar, A., Vandenberghe, D., Panaiotu, E.C., Panaiotu, C.G., Necula, C. Cosma, C., van den Haute, P., 2010. Optical dating of Romanian lœss using fine-grained quartz. Quaternary Geochronology 5, 143-148.

58- Timar-Gabor, A., Vandenberghe, D.A.G., Vasiliniuc, S., Panaiotu, C.E., Panaiotu, C.G., Dimofte, D., Cosma, C., 2011, Optical dating of Romanian loss: A comparison between silt-sized and sand-sized quartz. Quaternary International 240, 62-70.

59- Tonov, Ch., Vangelova, V., Vangelov, D., 2016. Mineralogy and geochemistry of kaolin deposits in Senovo – Vetovo and Kaolinovo region and notions of their genesis. Annals of the University of Sofia "St. Kl. Ohridski", Faculty of Geology and Geography, 1, 104, 43-64.

60- Vasiliniuc, S., Timar-Gabor, A., Vandenberghe, D.A.G., Panaiotu, C.G., Begy, R.C.S., Cosma, C., 2011. A high-resolution optical dating study of the Mostiştea loess-paleosol sequence (SE Romania) using sand-sized quartz. Geochronometrica 38 (1), 34-41.

61- Vasiliniuc, S., Vandenberghe, D.A.G., Timar-Gabor, A., Panaiotu, C., Cosma, C., van den Haute, P., 2012, Testing the potential of elevated temperature post-IR IRSL signals for dating Romanian loess. Quaternary Geochronology 10, 75-80.

675 62- Vasiliniuc, S., Vandenberghe, D.A.G., Timar-Gabor, A., Van Den haute, P., 2013.
676 Conventional IRSL dating of Romanian loess using single aliquots of polymineral fine
677 grains. Radiation Measurements 48, 60-67.
678 63- Yi, S. Buylaert J.-P., Murray, A.S., Lu, H., Thiel, C., Zeng, L. 2016. A detailed post-IR
679 IRSL dating study of the Niuyangzigou loess site in northeastern China. Boreas 45, 644-657.
680 64- Zagorchev, I., 2009. Geomorphological zonation of Bulgaria. Principles and state of the art.
681 Proceedings of the Bulgarian Academy of Sciences 62 (8), 981- 992.
682 65- Zeeden, C., Kels, H., Hambach, U., Schulte, P., Protze, J., Eckmeier, E., Markovic, S.B.,
683 Klasen, N., Lehmkuhl, F. 2016. Three climatic cycles recorded in a loess-palaeosol sequence
684 at Semlac (Romania). Implications for dust accumulation in south-eastern Europe.
685 Quaternary Science Reviews 154, 130-142.
686 66- Zeeden, C., Hambach, U., Veres, D., Fitzsimmons, K., Obrecht, I., Bosken, J., Lehmkuhl,
687 F., 2018. Millennial scale climate oscillations recorded in the Lower Danube loess over the
688 last glacial period. Palaeogeography, Palaeoclimatology, Palaeoecology 509, 164-181.
689
690
691 **Captions**
692
693 Figure 1A. Loess distribution in Europe and location of the study area.
694
695 Figure 1B. Location of the sampling sites and sites mentioned in the text.
696
697 Figure 2. Loess-paleosol sequences from NE Bulgaria and SE Romania.
698 Lithostratigraphy: L= loess deposit; S: soil and palaeosol.
699
700 Figure 3. Comparative dose response curves of the $pIRIR_{290}$ signal observed for samples VIA2
701 (L2), VIA3 (L3) and VIA7 (L7). The inset shows the natural decay curve of the $pIRIR_{290}$
702 signal.
703 Curves are fitted with a single saturating exponential function; VIA2 (L2): 2Do=704; VIA3 (L3): $2D_0$=718;
704 VIA7 (L7): $2D_0$=683.
705
706 Figure 4. $IRSL_{50°C}$ additive growth curves obtained for samples VIA3 (L3) and VIA7 (L7).
707 Curves are fitted with a single saturating exponential function; VIA3 (L3): $2D_0$=1386; VIA7 (L7):
708 $2D_0$=1466.
709
710 Figure 5. Comparative magnetic susceptibility records of the SE Romanian and
711 NE Bulgarian loess sequences.
712 Gray circles: IRSL samples from Balescu et al. (2010); white circles : IRSL samples from the
713 present study.
714 References: Mostiştea (Panaiotu et al., 2001); Mircea Vodă (Timar et al., 2010); Koriten (Jordanova and
715 Petersen, 1999a,b) ; Viatovo (Jordanova et al., 2008) ; Kaolinovo (unpublished)
716
717 Table 1. Luminescence data for the Bulgarian loess
718
719
720

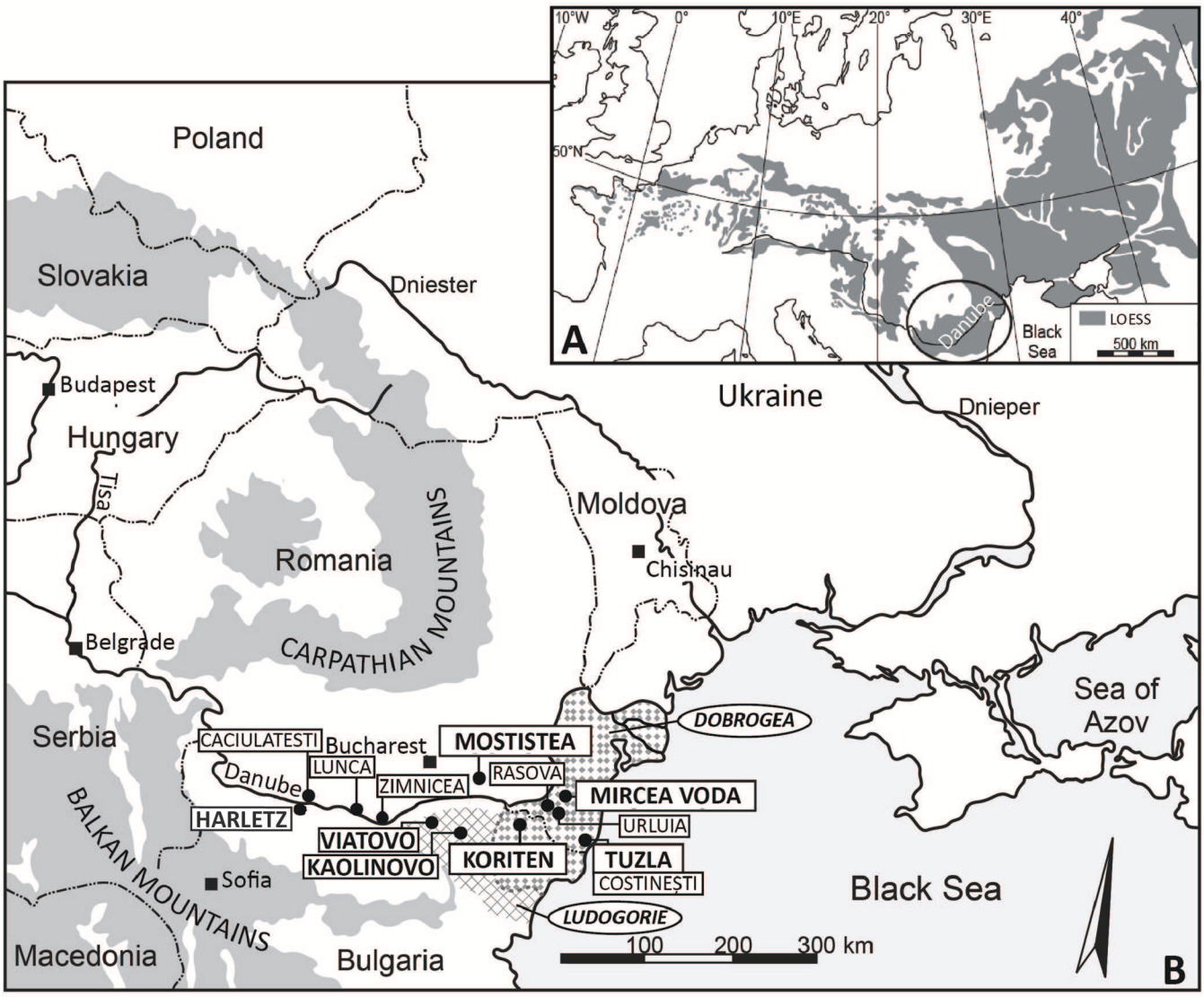
10°W
0°
10°E
20°
30°E
40°
50°N
A
Danube
Black Sea
LOESS
500 km
Poland
Slovakia
Dniester
Budapest
Hungary
Tisa
Ukraine
Dnieper
Moldova
Chisinau
Romania
CARPATHIAN MOUNTAINS
Belgrade
Serbia
Sea of Azov
DOBROGEA
CACIULATESTI
Bucharest
MOSTISTEA
LUNCA
RASOVA
Danube
ZIMNICEA
MIRCEA VODA
HARLETZ
URLUIA
VIATOVO
KAOLINOVO
KORITEN
TUZLA
COSTINEȘTI
Black Sea
BALKAN MOUNTAINS
Sofia
LUDOGORIE
Macedonia
Bulgaria
100
200
300 km
B

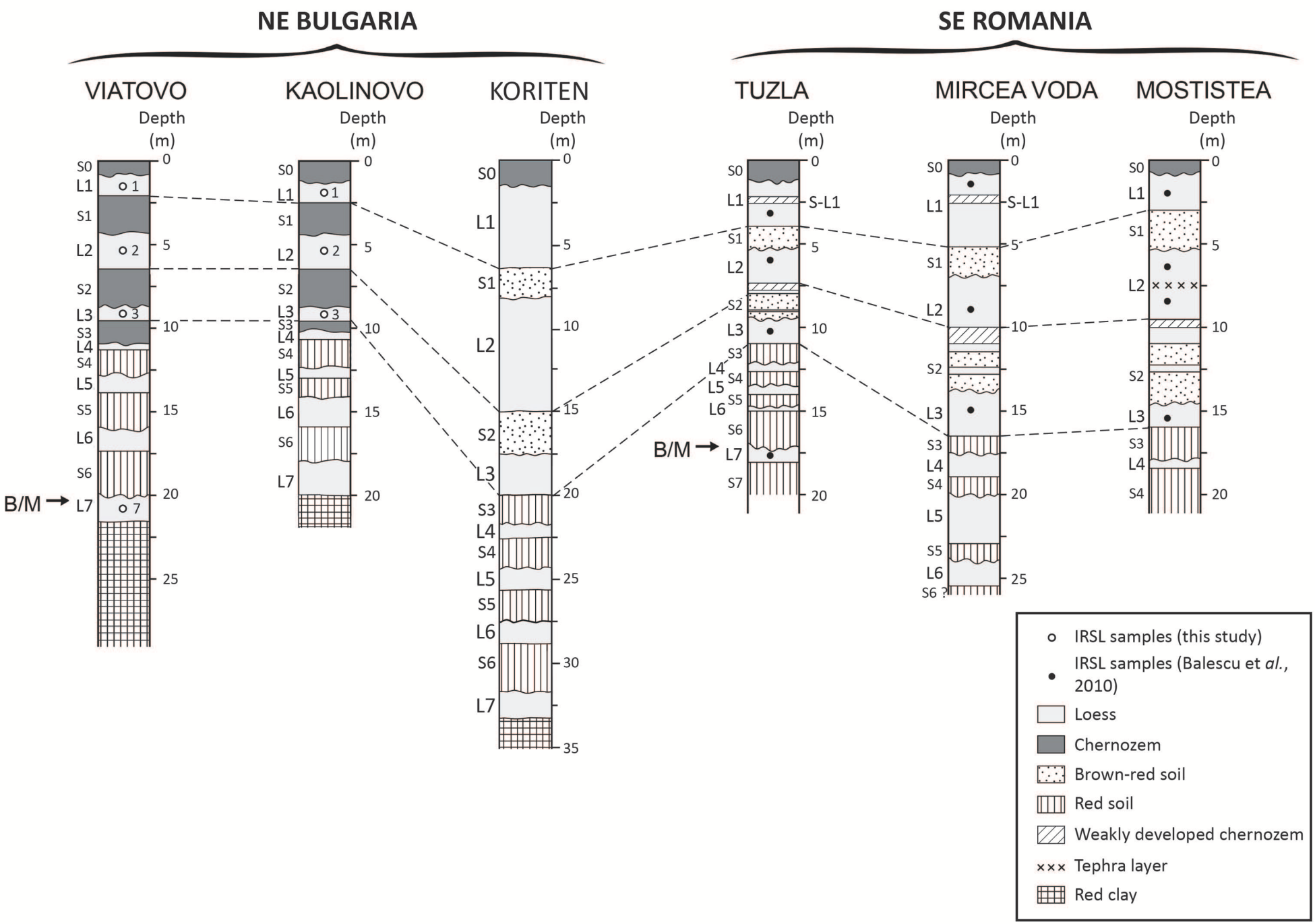
NE BULGARIA
SE ROMANIA
VIATOVO
KAOLINOVO
KORITEN
TUZLA
MIRCEA VODA
MOSTISTEA
Depth (m)
B/M
S-L1
S6 ?
IRSL samples (this study)
IRSL samples (Balescu et al., 2010)
Loess
Chernozem
Brown-red soil
Red soil
Weakly developed chernozem
Tephra layer
Red clay

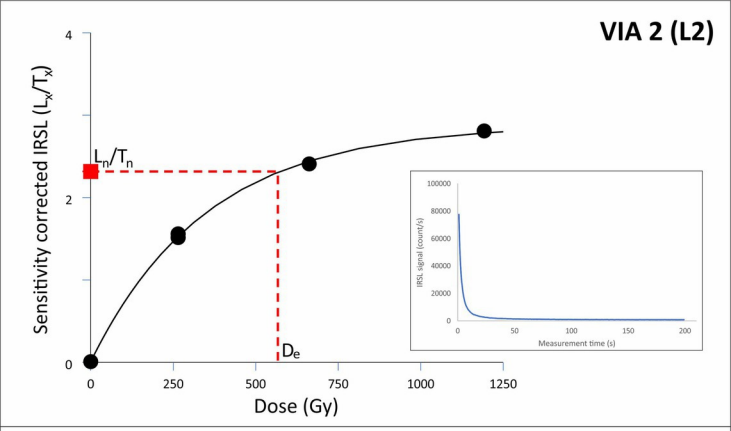
VIA 2 (L2)
Sensitivity corrected IRSL (L_x/T_x)
L_n/T_n
D_e
Dose (Gy)
IRSL signal (count/s)
Measurement time (s)

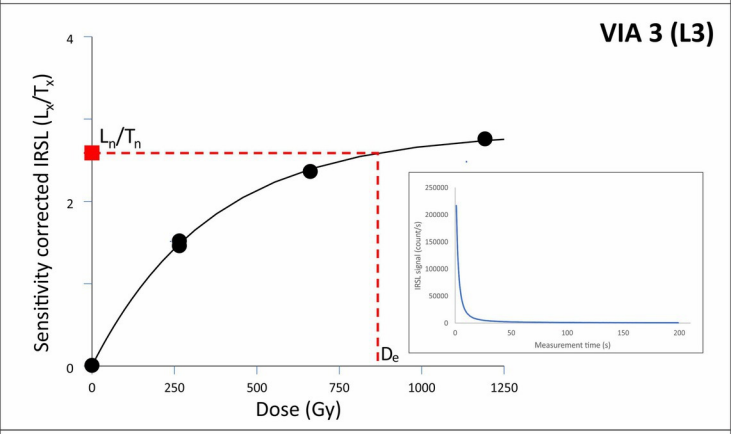
VIA 3 (L3)
Sensitivity corrected IRSL (L_x/T_x)
L_n/T_n
D_e
Dose (Gy)
IRSL signal (count/s)
Measurement time (s)

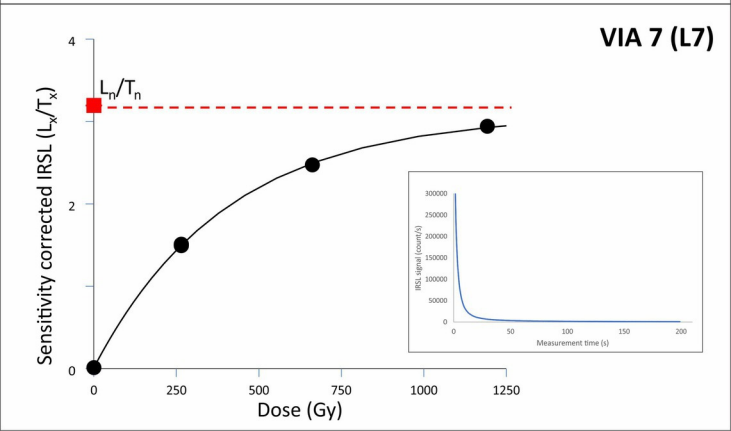
VIA 7 (L7)
Sensitivity corrected IRSL (L_x/T_x)
L_n/T_n
Dose (Gy)
IRSL signal (count/s)
Measurement time (s)

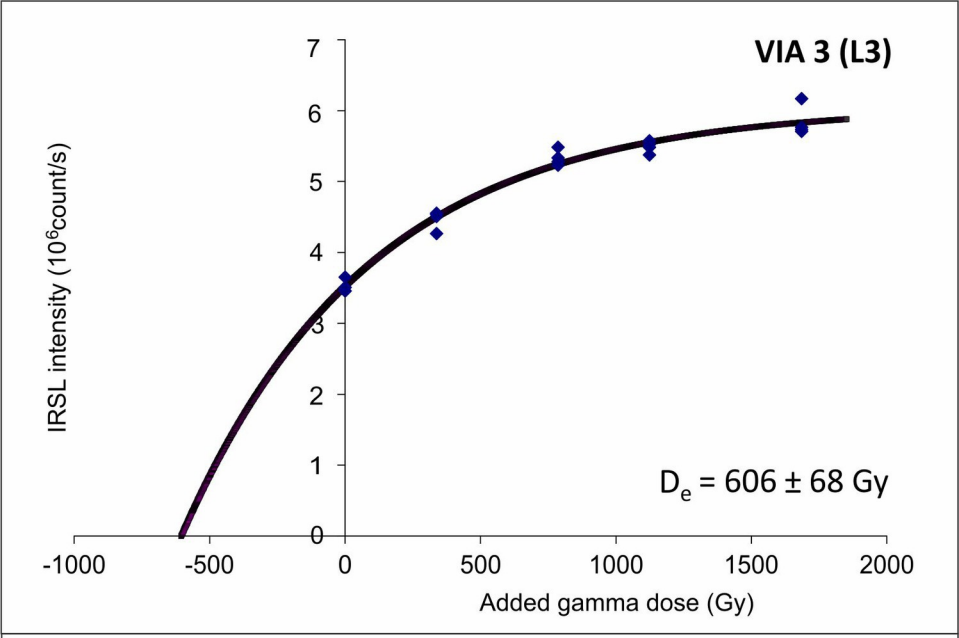
VIA 3 (L3)
IRSL intensity (10^6count/s)
7
6
5
4
3
2
1
0
-1000
-500
0
500
1000
1500
2000
Added gamma dose (Gy)
D_e = 606 ± 68 Gy

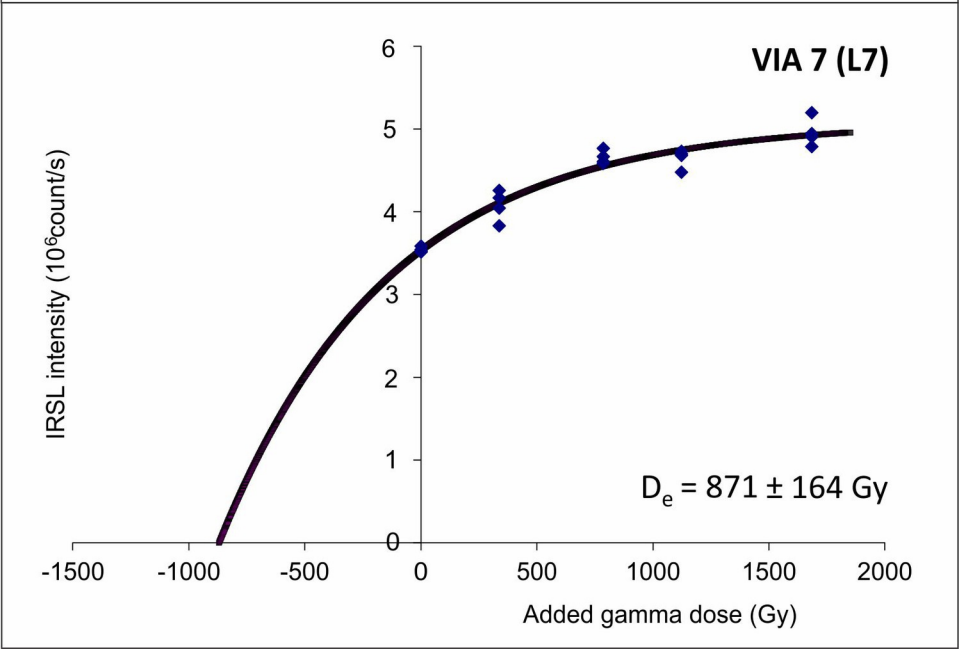
VIA 7 (L7)
IRSL intensity (10^6count/s)
6
5
4
3
2
1
0
-1500
-1000
-500
0
500
1000
1500
2000
Added gamma dose (Gy)
D_e = 871 ± 164 Gy

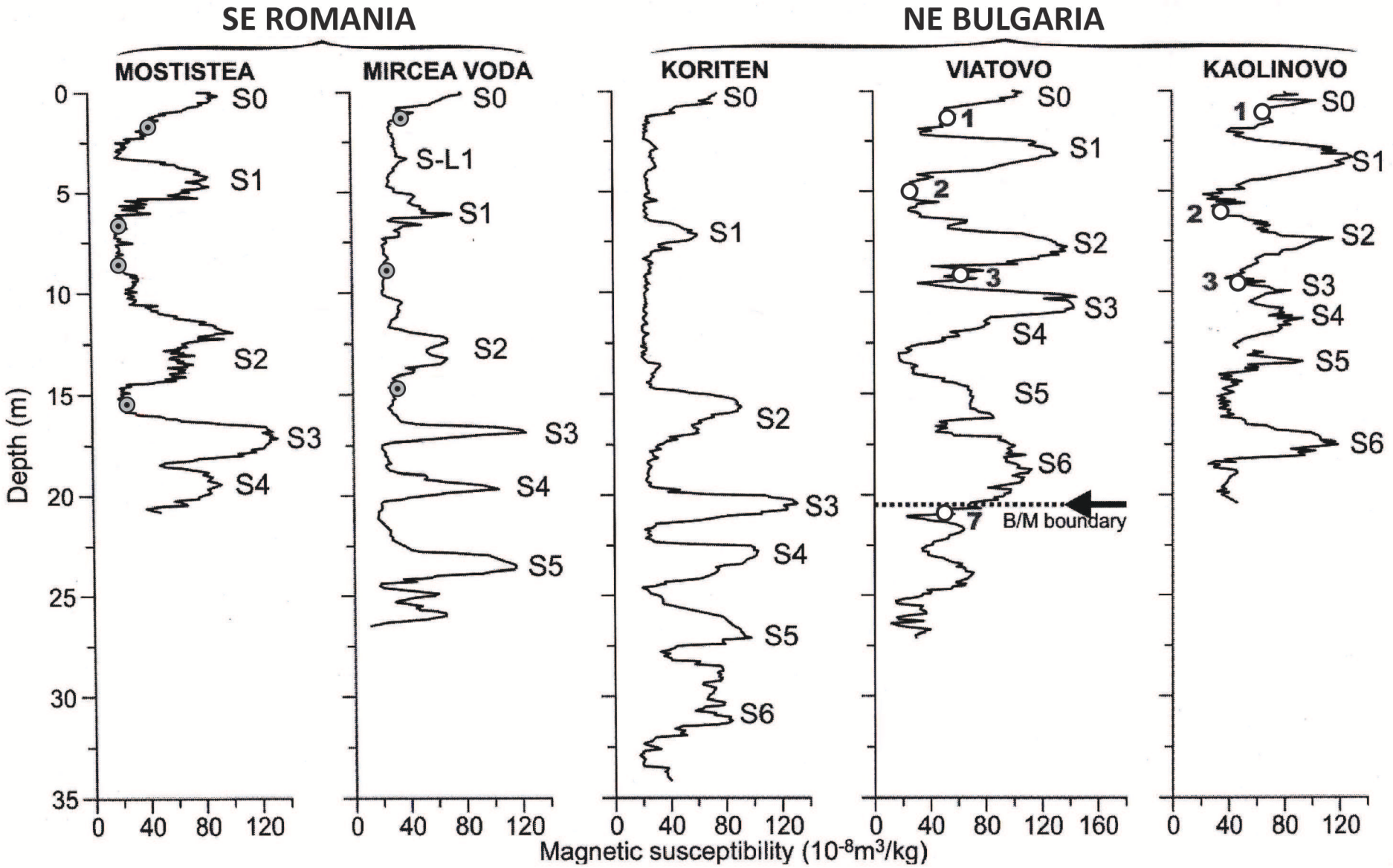
SE ROMANIA
NE BULGARIA
MOSTISTEA
MIRCEA VODA
KORITEN
VIATOVO
KAOLINOVO
Depth (m)
S0
S1
S2
S3
S4
S5
S6
S-L1
1
2
3
7
B/M boundary
0
5
10
15
20
25
30
35
0 40 80 120
0 40 80 120 160
Magnetic susceptibility (10-8m3/kg)

Site	Sample	Loess unit	Technique	Measured De (Gy)	Da (Gy/ka)	Measured ages: MAAD $IRSL_{50}$ and PIR-IR_{290} (ka ±σ)	Corrected ages: MAAD $IRSL_{50}$ (ka ±σ)	2Do	Chrono strati graphy
Viatovo	VIA 1	**L1**	MAAD-$IRSL_{50}$	182 ± 8	3.22 ± 0.13	57 ± 5	**60 ± 5**	1136	M I S 2- 4
			PIR-IR_{290}	205 ± 5	3.22 ± 0.13	**64 ± 5**	**-**	741	
	VIA 2	**L2**	MAAD-$IRSL_{50}$	442 ± 25	3.18 ± 0.13	139 ± 12	**167 ± 14**	1322	M I S 6
			PIR-IR_{290}	572 ± 6	3.18 ± 0.13	**180 ± 9**	**-**	726	
	VIA 3	**L3**	MAAD-$IRSL_{50}$	606 ± 68	2.97 ± 0.12	204 ± 26	**285 ± 35**	1386	M I S 8
			PIR-IR_{290}	871 ± 37	2.97 ± 0.12	**293 ± 17**	**-**	694	
	VIA 7	**L7**	MAAD-$IRSL_{50}$	871 ± 164	2.94 ± 0.12	296 ± 60	**>1066**	1466	> B/M ~780 ka
			PIR-IR_{290}	saturated	2.94 ± 0.12	**Infinity**	**-**	736	
Kaolinovo	KA 1	**L1**	MAAD-$IRSL_{50}$	218 ± 10	5.13 ± 0.18	42 ± 3	**44 ± 3**	1428	M I S 2-4
			PIR-IR_{290}	228 ± 5	5.13 ± 0.18	**45 ± 2**	**-**	550	
	KA 2	**L2**	MAAD-$IRSL_{50}$	516 ± 77	3.43 ± 0.13	150 ± 25	**184 ± 29**	1458	M I S 6
			PIR-IR_{290}	573 ± 13	3.43 ± 0.13	**167 ± 7**	**-**	746	
	KA 3	**L3**	MAAD-$IRSL_{50}$	638 ± 151	3.33 ± 0.13	192 ± 48	**264 ± 64**	1364	M I S 8
			PIR-IR_{290}	986 ± 43	3.33 ± 0.13	**296 ± 17**	**-**	722	

Table 1